Journal of Electroanalytical Chemistry 741 (2015) 1–7

Contents lists available at ScienceDirect

Journal of Electroanalytical Chemistry

journal homepage: www.elsevier.com/locate/jelechem

The dissolution of palladium as a function of glucose concentration in chloride containing solutions of acidic pH

Matthias Gerstl [a,*], Martin Joksch [b], Guenter Fafilek [a,c]

[a] Austrian Centre of Industrial Biotechnology (ACIB), A-8010, Austria
[b] Siemens AG, A-1211, Austria
[c] Vienna University of Technology (VUT), A-1060, Austria

ARTICLE INFO

Article history:
Received 1 October 2014
Received in revised form 7 January 2015
Accepted 10 January 2015
Available online 20 January 2015

Keywords:
Non-enzymatic glucose detection
Palladium electrode
Cyclic voltammetry
Dissolution of palladium

ABSTRACT

A strong anodic peak observed in cyclic voltammetry measurements of palladium electrodes when adding glucose to chloride containing (0.1 M) slightly acidic (pH 5.3) unbuffered media was studied in detail. The peak was highly sensitive to glucose concentration (5–20 g/L). Experiments were conducted by variation of pH (1–13) and chloride concentration (0.5–50 g/L) of the medium over a wide range, as well as substituting chloride with bromide. The resulting data suggests dissolution of the electrode as a chloride complex as the root cause for the peak, which is triggered by the addition of glucose to the electrolyte. The organic substances are oxidised thereby removing the protecting oxide layer and enabling the dissolution. This reaction is only observed in a certain window confined by both pH and halide concentration.

1. Introduction

The search for a reliable, cheap, fast and precise method to quantify glucose in solution has been going on for decades [1], with the main incentive being the hope of improvement in the treatment of the widespread disease diabetes mellitus, suffered by millions around the globe. Today the state of the art in glucose monitoring is enzymatic oxidation of glucose with amperometric detection of the reaction products or even direct transfer of the redox current to the electrode [2–7]. However, considerable effort is being made to develop a new generation of so-called non-enzymatic glucose sensors, which promise a longer lifetime and cheaper manufacturing and handling [2–5,7]. These sensors usually consist of a combination of one or more metals or carbon species, recent examples include Au [8–10], boron doped diamond [11], Cu [12], Ni [13], Pd [14–16] or Pt [16,17], which are very often nano structured. Comprehensive reviews following the progress of these developments are published every few years, but commercialization is yet to be achieved [2–5,7]. High chloride content of human blood and interference of other redox active species have been identified as the main obstacle [10]. Most of the work on model systems has been done in basic media, as glucose is more readily oxidised at higher pH, down to the pH of blood of 7.4 [18–21].

Besides blood sugar measurement other areas would also benefit of reliable non-enzymatic glucose sensors such as fermentation monitoring. In this area usually a multitude of different types of sensors is utilised to measure an array of properties to predict the present state of the fermentation process and, if needed, make adjustments [6,22–28]. While some parameters are easily measured and controlled, such as temperature, pH value or oxygen partial pressure, it is highly desirable to have a method that additionally measures concentrations of dissolved components, as the available solutions are usually expensive and high maintenance [5]. Glucose is a common nutrient in industrial fermentations and having a cheap and fast means to determine it is highly desirable.

However, results from the research on blood sugar sensors are often not easily transferable to the fermentation research, as the solution composition is different and changing. Also the fermentation medium may be acidic and the research on glucose oxidation in acidic media, especially in chloride containing electrolytes, is sparse with notable exceptions [12].

Nonetheless, in a previous study we showed that by using cyclic voltammetry a simple polycrystalline palladium electrode exhibits a strong sensitivity to glucose in a model yeast fermentation medium of pH 5.3 and about 0.1 M Cl^- concentration [29]. In this contribution we aim to clarify the reaction mechanism of this unexpected result.

* Corresponding author.
E-mail address: matthias.gerstl@tuwien.ac.at (M. Gerstl).

http://dx.doi.org/10.1016/j.jelechem.2015.01.009
1572-6657/

2. Experimental

Palladium and Platinum wires of 100 μm diameter, as well as a palladium sheet and target and a titanium sheet electrode were purchased from Oegussa (Vienna, Austria) with a purity of 99.99%.

Micro Electrodes were prepared by leading metal wires through a glass capillary and sealed using a capillary puller (Model PP-830, Narishige, Japan) and manually polished in steps to grit 4000 (SiC Paper, Struers, Denmark). The palladium sheet was partially covered with lacquer (Abdecklack Rot, Metallchemie GesmbH, Austria) to ensure that always the same electrode area of 0.7 cm^2 was used.

Thin palladium layers were prepared on a polycrystalline titanium electrode by magnetron sputtering (Med020, Bal-Tec, Liechtenstein) in 2×10^{-2} mbar Ar pressure with a sputter current of 100 mA for 150 s. The Ti surface not covered with Pd was painted with lacquer. The area covered with Pd was 2.2 cm^2. Thickness of the deposited layer was approximately 100 nm, estimated by comparing to sputter times of platinum and gold.

The test solutions were prepared by dissolving either sodium chloride, potassium bromide or sodium sulphate in deionised water. The pH was adjusted using diluted hydrochloric acid for the chloride containing solution or sulphuric acid for the chloride free medium, as well as diluted sodium hydroxide with the aid of a Metrohm 827 pH electrode (Metrohm, CH). Glucose was subsequently added as glucose monohydrate and was obtained from Merck, Germany. The solutions were deliberately unbuffered and not deaerated to mimic a real filtered fermentation solution. All chemicals were purchased from Merck, Germany and were of p.a. grade.

Cyclic voltammograms were recorded on an Autolab PGSTAT 128 N using the Nova 1.10 software (both Metrohm Autolab, Utrecht, The Netherlands) at ambient temperature of 22 °C; the temperature was not controlled further. A saturated Mercury sulphate electrode (SMSE) was used as a reference electrode, with a potential of +0.65 V versus the standard hydrogen electrode (SHE). Measurements were recorded until stable voltammograms were achieved, which took usually 20 scans, the last of which is shown in the corresponding graphs. No further electrochemical pretreatment was performed and the scan rate and potential range were not changed during scans. Prior to the measurements the electrodes were rinsed with deionized water. Exact parameters of the individual measurements are given in the figure captions.

Potentials in the text are, except noted otherwise, given with reference to the reversible hydrogen electrode RHE. In the figures the voltammograms are plotted versus the RHE as well as the standard hydrogen electrode (SHE). The potentials were calculated according to

$$E(SHE) = E(SMSE) + 0.65$$

and

$$E(RHE) = E(SHE) + 0.059 \times pH.$$

The current of the cyclic voltammograms is normalised to the geometric area of the electrodes.

3. Results and discussion

3.1. General characteristics and comparison of Pt and Pd electrodes

In Fig. 1(a) and (b) cyclic voltammograms of platinum and palladium microelectrodes in a sulphate electrolyte with and without 0.11 M (20 g/L) Glucose at pH 5.3 are plotted. The electrochemical reactions taking place at the interface of the platinum electrode have been treated in detail in the literature [2,3,18,19,21,30], but warrant a short recap, by reference to Fig. 1(a).

In the so called hydrogen region, marked with 1, the chemisorption of glucose takes place by dehydrogenation of the hemi-acetalic carbon atom at the C1 position [3,19,30], while in the base electrolyte the cathodic current is caused by reduction of dissolved oxygen [31]. Peak 2 is due to the oxidation of the chemisorbed glucose in the region with adsorbed OH_{ads}-ions, which start to form in this voltage regime [3,19] and coincides with the stop of oxygen reduction in the base electrolyte and the beginning of platinum oxidation. With further anodic polarisation the OH_{ads} species is first oxidised to O_{ads}, which is less active towards the oxidation reaction, until a PtO film is formed. This oxide film enables the direct oxidation of glucose, which is the cause of peak 3, further oxidation of Pt inhibits this reaction [3,19]. The first notable feature in the cathodic sweep is peak 4, which indicates the start of the surface reduction of platinum. This is immediately followed by the sharp anodic peak 5. This feature has been attributed to chemisorption and dehydrogenation of glucose on the just freed up surface [19], or, in alkaline media, to oxidation of adsorbed gluconolactone to gluconate [30].

It is noteworthy that the palladium electrode in Fig. 1(b) is by far an inferior catalyst towards the oxidation of glucose than the platinum electrode is. However, at a first glance the general reaction scheme seems to be similar in some respects and will be treated in the next section.

Fig. 1(c) and (d) show the cyclic voltammograms of above Pt and Pd microelectrodes in a chloride electrolyte with and without addition of glucose. When comparing Fig. 1(a)–(c) it is immediately obvious that the total oxidation current of the platinum electrode dramatically drops in the chloride electrolyte. This is also a well described effect, caused by the chemisorption of chloride ions at the Pt surface which inhibits the formation of an OH_{ads} film, which is integral in the oxidation of glucose, as well as other organic substances and carbon monoxide [19,20,32].

Finally the comparison between cyclic voltammograms of the palladium electrode in the chloride free and chloride containing electrolyte shown in Fig. 1(b) and (d) yields an unexpected result: An additional peak, marked with an arrow in Fig. 1(d), appears in the chloride containing medium with the addition of glucose. However, even in the base electrolyte the anodic current is significantly higher in this region, when compared to the chloride free medium. The peak position is overlapping with peak 2 in Fig. 1(a), however, it is highly unusual that no such prominent feature is visible in the chloride free medium. To gain further understanding of the glucose oxidation on palladium a more in depth study is presented in the following sections.

3.2. Glucose oxidation on palladium in chloride free medium

In Fig. 2 cyclic voltammograms of a palladium sheet electrode in chloride free glucose solutions of different concentrations are compared. The numbered features can be reasonably explained by reference to literature studies. In analogy to the reaction on platinum peak 1 can be attributed to the initial dehydrogenation and adsorption of glucose to the palladium surface in the double layer region [33].

Peak 2 marks the onset of palladium oxidation in the glucose free medium, better visible in the inset of Fig. 2, commonly associated with PdOH formation [34–36]. Notably, in contrast to the Pt electrode in Fig. 1(a), no anodic signal connected to glucose addition can be discerned at peak 2.

The onset of peak 3 coincides well with the formation potential of $Pd(OH)_2/PdO$ in the Pourbaix diagrams in Fig. 4. Thus, the additional anodic current upon glucose addition is readily explained by the direct reaction of glucose with palladium oxide [33] analogous

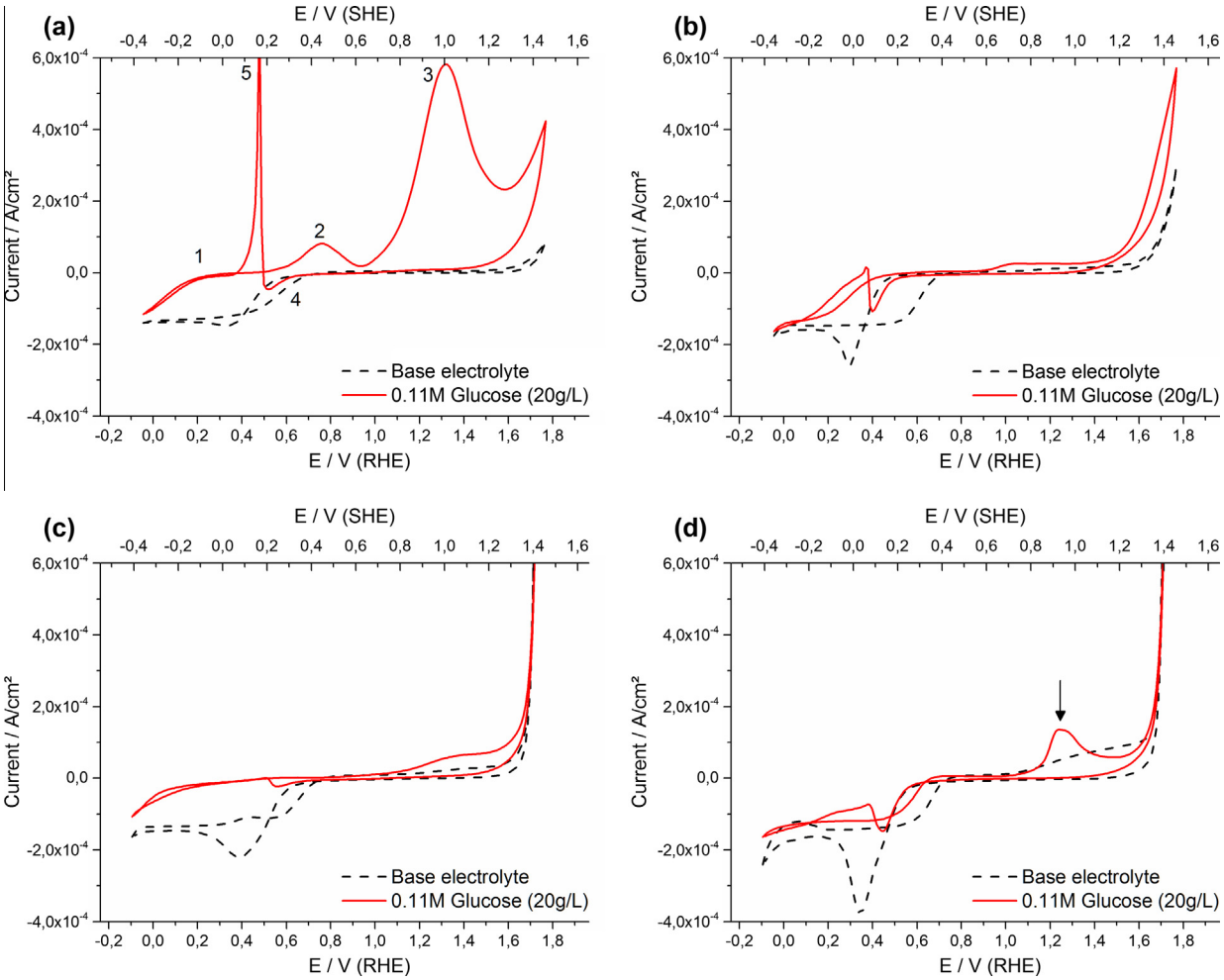

Fig. 1. Cyclic voltammetry at 100 µm diameter micro electrodes in an electrolyte with (solid red line) or without (dashed black line) 20 g/L (112 mM) glucose at pH 5.3. Scan rate 10 mV/s. (a) Pt in 29 mM Na_2SO_4 electrolyte; (b) Pd in 29 mM Na_2SO_4 electrolyte; (c) Pt in 86 mM (5 g/L) NaCl electrolyte; d) Pd in 86 mM (5 g/L) NaCl electrolyte. Salt concentrations were chosen to represent the same ionic strength. Numbers in (a) are referred to in the text, the arrow in (d) marks the anomalous peak. (For interpretation of the references to colour in this figure legend, the reader is referred to the web version of this article.)

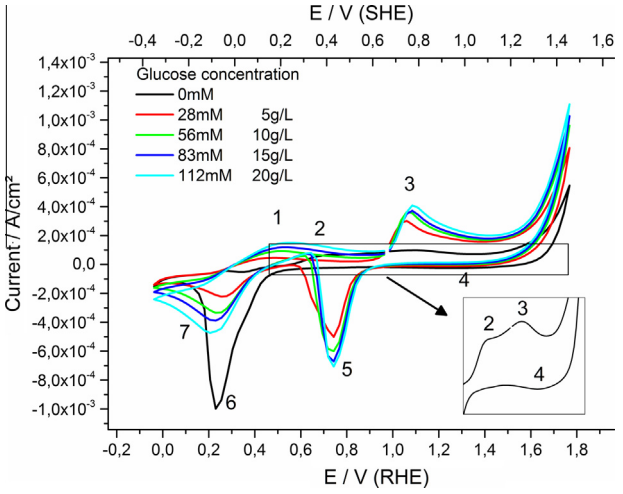

Fig. 2. Cyclic voltammetry at a Pd sheet electrode in a 29 mM Na_2SO_4 electrolyte with different glucose concentrations. Scan rate 100 mV/s. The numbers are referred to in the text. The inset shows the area of the graph highlighted in the box.

to the situation on platinum [3,19]. With further polarisation a monolayer of PdO is formed at about 1.4–1.5 V vs RHE and the reaction attenuates [36,37].

In the cathodic run the faint peak 4, better visible in the inset in Fig. 2, has been ascribed to the reduction of palladium IV oxide, formed in the close to and beyond the oxygen evolution reaction at the maximum anodic potential [34,38]. This feature is only visible in the glucose free medium.

Peaks 5 and 6 are caused by the reduction of the surface oxide layer. It is a curious effect that without glucose, the reduction happens at a significantly more negative potential, cf. peak 6. These features are best explained with the α/β oxide model. The α-oxide is a two-dimensional compact layer of a few monolayers of PdO and PdO_2, while the β-oxides are of columnar shape and hydrous and consist of PdO_2. Both are reduced at different potentials depending on the electrochemical history of the electrode [39]. In the present case the β-oxide is preferentially formed without glucose, while the glucose containing solutions favour the α-oxide formation. It might be the case that the presence of glucose inhibits this formation of higher oxides. However, palladium oxide reduction has been acknowledged to be highly complex [34,39–41] and is not the focus of the present study.

Immediately cathodic of peak 5 another dehydrogenation peak is discernible, cf. peak 4 in Fig. 1(a). Finally, peak 7 corresponds to reverse reaction to peak 1.

3.3. Glucose oxidation on palladium in chloride containing medium

In Fig. 3 cyclic voltammograms of a palladium sheet electrode, recorded in a chloride containing medium with various glucose concentrations, are plotted. Compared to the reaction in the sulphate electrolyte in Fig. 2, almost no dehydrogenation and adsorption features are visible in region 1, with the exception of the faint anodic peak 7 in the cathodic sweep, note the arrow in Fig. 3. However, the first palladium oxidation step in region 2 is significantly reduced as soon as glucose is added to the solution. This would hint at an adsorption of glucose or its oxidation products without a redox reaction, inhibiting the PdOH formation.

As in the case of the palladium microelectrode in Fig. 1(d), the most striking feature is the anomalous anodic peak 3, which will be discussed thoroughly in a dedicated section.

In the cathodic sweep a reduction signal, peak 4, shortly after the positive turnaround potential is due to reduction of Cl_2 [42] and is only seen for glucose concentrations of 0 g/L and 5 g/L. The same holds true for the flat cathodic peak 5, which can be attributed to a reduction of higher palladium oxides, namely Pd^{4+} [34,38], see peak 4 in Fig. 2.

The reduction of the palladium oxide causes two peaks, both positions and intensities being dependent on the glucose concentration. Peak 6 seems to be equivalent to peak 5 in Fig. 2 and increases in current with glucose concentration. On the other hand, peak 8 decreases with glucose addition and shifts to more positive potentials, as indicated with the arrow close to peak 8. This behaviour is compatible with the explanation given in the discussion of Fig. 2, if one assumes a more gradual transition in the formation of the different oxides.

3.4. The origin of the anomalous peak

While a lot of features show up in Fig. 3, arguably the most interesting one is the large anodic peak 3. From an angle of a possible application as a glucose sensor, compared to Fig. 2 the sensitivity is about a factor 3 higher and works in an acidic and chloride containing medium.

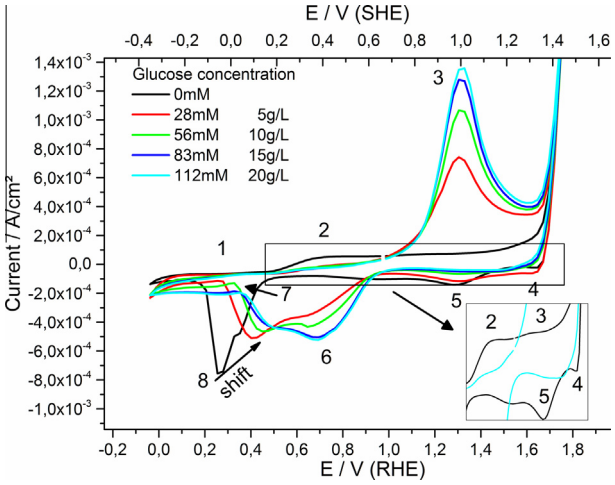

Fig. 3. Cyclic voltammetry at a Pd sheet electrode in a 86 mM NaCl electrolyte with different glucose concentrations. Scan rate 100 mV/s. The numbers are referred to in the text. The arrow at peak 7 highlights the barely visible peak, while the arrow at peak 8 indicates the shift of peak 8 with increasing glucose concentration. The inset shows the area of the graph highlighted in the box.

The onset of the anomalous peak coincides with the $PdOH_2$/PdO formation potential, which is better visible in the inset of Fig. 3. Therefore, it seems reasonable to assume that the underlying mechanism can be linked, at least partially, to direct glucose oxidation by PdO, cf. Fig. 2, even though the peak shape and maximum position is quite different. However, a look at the Pourbaix diagram in Fig. 4(a) shows that at pH 5.3 palladium dissolution as $[PdCl_4]^{2-}$ should also be expected around the formation of $Pd(OH)_2$. A dissolution reaction can certainly account for the high current, but does not explain the glucose concentration dependence.

To investigate possible effects on the glucose oxidation reaction and the role of electrode dissolution, pH and chloride concentration was varied systematically and corresponding cyclic voltammograms are plotted in Fig. 5(a)–(c). In agreement with the Pourbaix diagram in Fig. 4(a), the onset potentials of the anodic peak for pH values of 2 and 5.3, in Fig. 5(a) and (b) respectively, indeed shift to smaller values and higher currents with increasing Cl^- concentration.

However, at pH 2 the addition of glucose does not increase the already large anodic signal, see Fig. 5(a); analogous behaviour was also observed for pH 1, but is not shown here. This can be explained by the fact that for all Cl^- concentrations, the polarisation for $[PdCl_4]^{2-}$ dissolution is already quite large until $Pd(OH)_2$ is formed, cf. Fig. 4(a), the latter being considered essential on the one hand in the formation of a protective layer and on the other hand in the glucose oxidation reaction [19–21,40].

At pH 5.3, shown in Fig. 5(b), a clear difference is visible between the glucose free and glucose containing media. The most pronounced difference is again the large anodic peak at about 1.2–1.5 V, which appears in the glucose solution, and is shifted to the left with increasing chloride concentration. However, the anodic peak in 50 g/L NaCl is already quite strong even without glucose in the solution, hinting at significant dissolution of palladium already happening before addition of the sugar.

At pH 13 in Fig. 5(c) the picture is quite different. The first peak in the anodic sweep at about 1.0 V gets smaller with increasing chloride concentration and the onset potential shifts to the right, while the peak potential shifts left. This is in line with the common explanation that chloride adsorption is in competition with OH_{ad} formation on the Pd surface sites [32,42]. As $[PdCl_4]^{2-}$ formation is pH independent, see Fig. 4(a), the onset potential vs RHE shifts to the right with increasing pH. Therefore, one has to polarise to very high potentials of more than 1.4 V to see glucose specific signals amplified by higher chloride concentration. The fact that a double peak is visible might be connected to the formation of the Pd^{4+} oxide, which is expected in this polarisation regime.

By substituting the supporting electrolyte from sodium chloride to potassium bromide, the dissolution of the palladium electrode is also expected to shift to lower potentials, as plotted in the Pourbaix diagram in Fig. 4(b). The cyclic voltammograms recorded in the corresponding experiment compared in Fig. 5(d) show that this is indeed the case and the effect is not restricted to chloride electrolytes. In fact the curves for both electrolytes look very similar aside from the earlier onset of halogen gas formation in the bromide solution and a corresponding stronger reduction peak of the Br_2. However, it is worth noticing that the end potential of the anomalous peak in the bromide electrolyte is also shifted to lower values and roughly coincides with the maximum of the anomalous peak in the chloride containing medium. Therefore, if the passivation mechanism is identical, the oxide monolayer forms at this lower potential in the bromide solution.

As a further means to study the role of palladium dissolution, thin Pd layers on a titanium substrate were used as an electrode and measured over an extended period of time. The obtained cyclic voltammograms are compared in Fig. 6. Due to the highly active surface of the sputtered palladium layer, the first cycles show

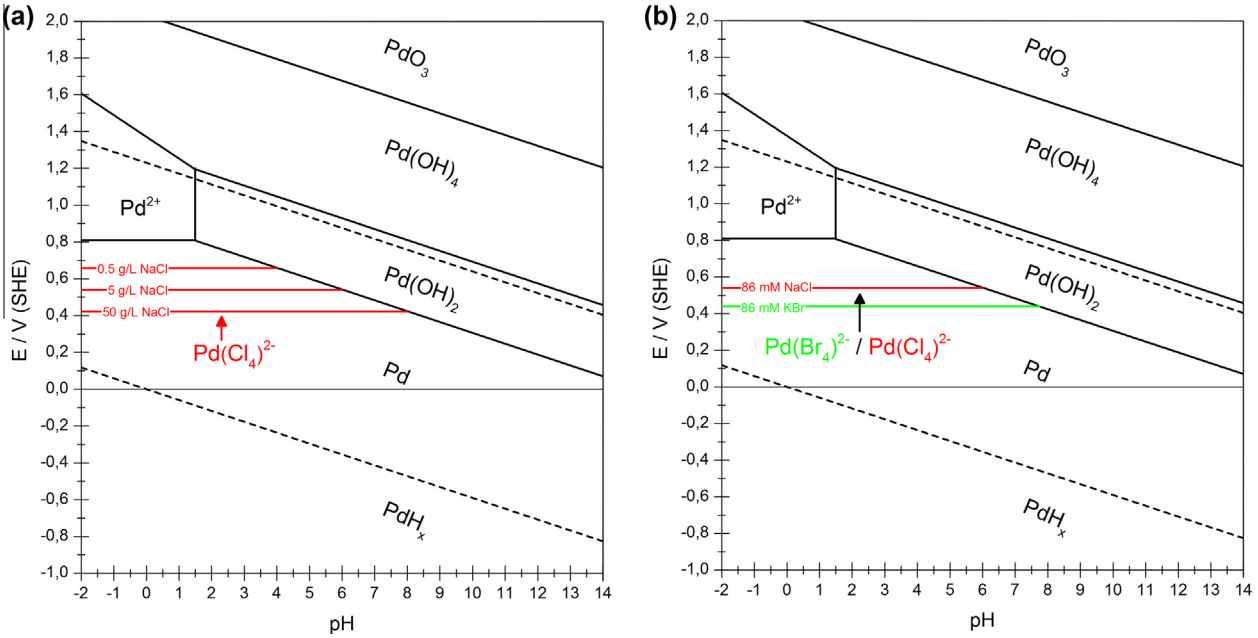

Fig. 4. Pourbaix diagrams for the system Pd-H_2O at 25 °C with overlays for the onset of halide complex corrosion: (a) different concentrations of NaCl; (b) comparison between NaCl and KBr corrosion. All soluble species at 1 μM. Data reconstructed from Refs. [43–46].

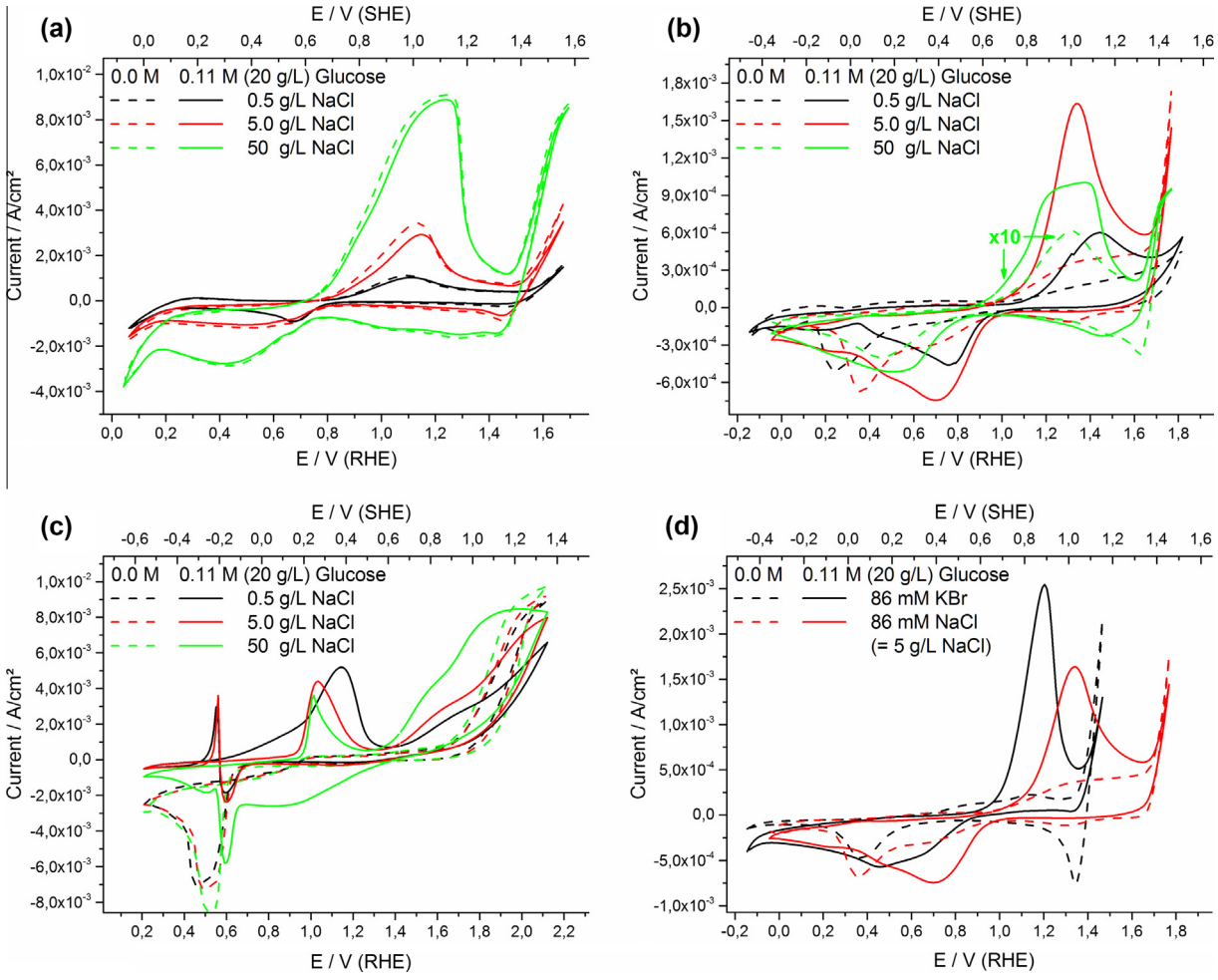

Fig. 5. Cyclic voltammetry at a Pd sheet electrode in different concentrations of a sodium chloride electrolyte with 112 mM glucose (solid lines) or without (dashed lines). (a) pH 2; (b) pH 5.3; (c) pH 13; (d) comparison of 86 mM KBr to 86 mM NaCl electrolyte in pH 5.3. The arrows in (b) indicate that the current for 50 g/L NaCl is an 10 times larger than shown. Scan rate 100 mV/s.

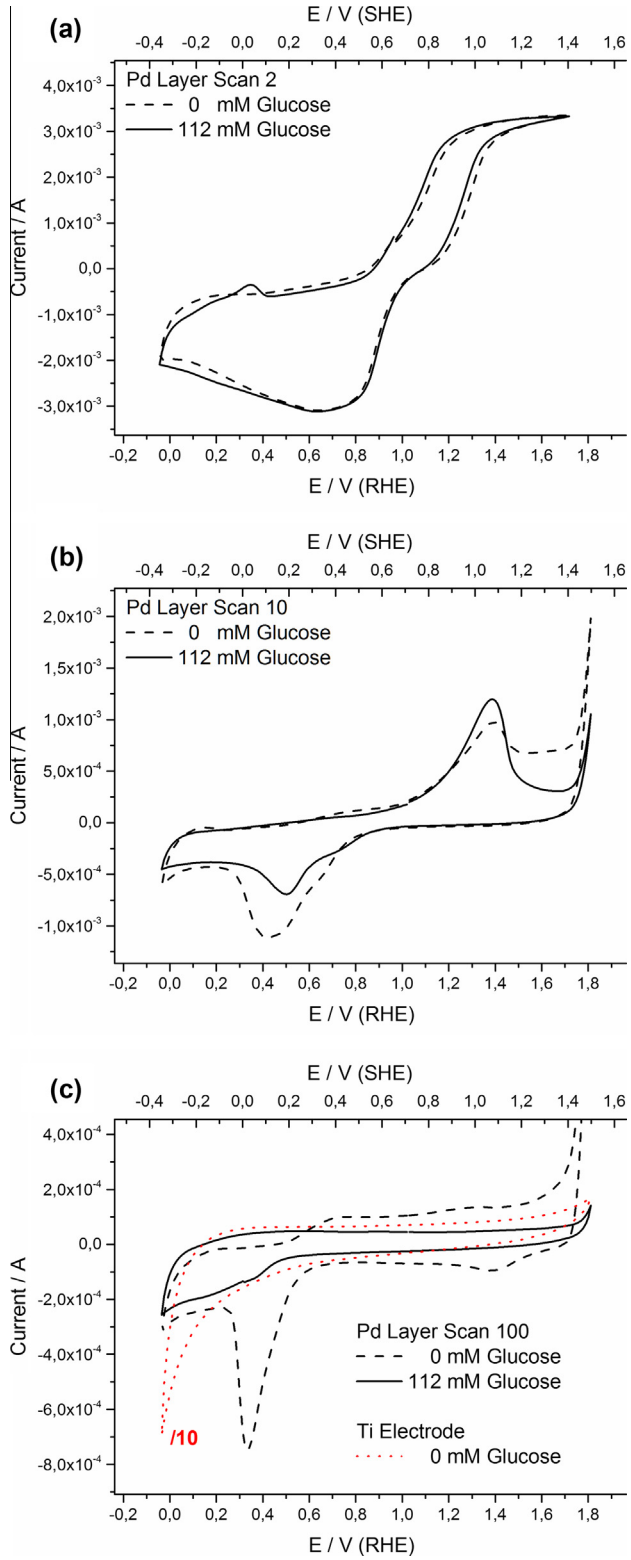

Fig. 6. Cyclic voltammetry at an approximately 100 nm thin Pd layer on a Ti substrate in a 86 mM NaCl electrolyte at pH 5.3, without (dashed lines) and with (solid lines) 112 mM glucose (20 g/L). Different scans are shown from the long term measurement: (a) scan 2; (b) scan 10; (c) scan 100. In (d) the dotted red line shows the voltammogram of a plain Ti electrode for comparison, the current has been augmented tenfold for visibility. Scan rate 100 mV/s. (For interpretation of the references to colour in this figure legend, the reader is referred to the web version of this article.)

strong anodic currents at potentials higher than about 1.0, due to dissolution of Pd. In the cathodic sweep the soluble $[PdCl_4]^{2-}$ complex is reduced starting at ca. 0.9 V. As an example the cyclic voltammogram of the second scan is shown in Fig. 6(a).

After about 10 scans, cf. Fig. 6(b), the CV of the palladium layer in the glucose containing solution looks very similar to the Pd sheet electrode in Fig. 3, exhibiting the strong anodic peak at 1.4 V. In the medium without glucose the peak is also visible, albeit weaker.

Finally after 100 scans, the Pd layer in the glucose solution has been completely dissolved and the CV looks very similar to that of a plain titanium electrode, see Fig. 6(c). However, in the glucose free solution a stable voltammogram is measured, as one would expect for palladium, without any further dissolution. Indeed, the latter CV looks very similar to the data measured in 0 g/L glucose shown in Fig. 3.

3.5. Proposed reaction mechanism

Based on the above data, as a working hypothesis, the reaction mechanism for the generation of the anomalous peak is suggested and sketched in Fig. 7.

If, depending on halogenide concentration and pH of the solution, the onset potential of palladium dissolution and palladium oxidation is reasonably close, palladium dissolution can be triggered by addition of simple organic substances like glucose.

In the absence of said organics, surface oxidation of palladium passivates the electrode and protects it against dissolution, see Fig. 7(a). However, highly active surfaces like freshly sputtered palladium will be dissolved initially regardless until the surface is sufficiently aged.

In the presence of adsorbed glucose the surface oxide is, at least partially, consumed in the glucose oxidation reaction, Fig. 7(b), and allows the attack and subsequent dissolution of the freed up palladium surface by halogenide complexing Fig. 7(c) and (d). At more positive potentials the formation of a dense palladium oxide monolayer stops the dissolution [36].

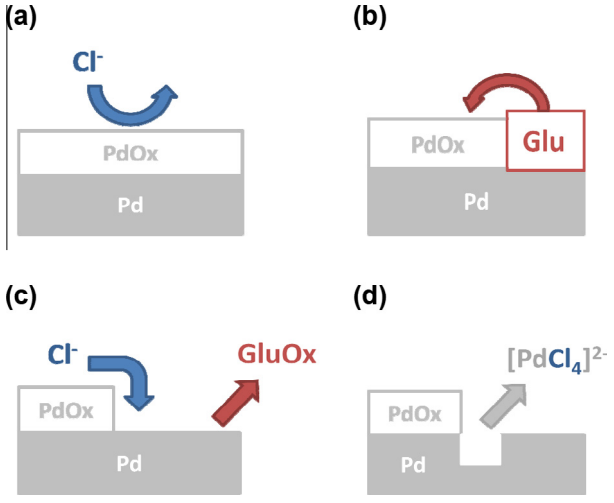

Fig. 7. Graphic representation of the proposed reaction mechanism for Pd dissolution triggered by glucose addition, valid only in the right pH and halide concentration region. (a) The surface oxide layer protects palladium from the dissolution by chloride. (b) Glucose, adsorbed at lower potentials, consumes the surface oxide. (c) Chloride attacks immediately after the oxidised glucose desorbs. (d) Palladium is dissolved as a chloride complex.

If the acidity of the solution is too strong, in the case of about 100 mM chloride below approximately pH 4, the polarisation and therefore rate for the halogenide complex formation is high when the glucose oxidation reaction would commence. Therefore, only dissolution of the electrode takes place and the sensitivity for the glucose concentration is lost.

4. Conclusion

An extensive study using cyclic voltammetry has been carried out in order to clarify the origin of an intensive anodic peak observed in the positive potential sweep in a glucose containing, unbuffered chloride electrolyte of pH 5.3 on a poly-crystalline palladium sheet electrode.

The peak intensity is highly sensitive to glucose and increasing with higher sugar concentrations. The onset potential of the peak shifts to lower values with higher chloride concentration and by exchanging chloride ions in the electrolyte with bromide. Below a certain pH, roughly pH 4 for 0.1 M Cl^-, the sensitivity for glucose is lost and a strong anodic peak is observed regardless of the glucose concentration. On the other hand, at a high pH of 13 chloride has an adverse effect on the glucose sensitivity of the Pd electrode, except at very high potentials.

The above properties can be explained by attributing dissolution of the palladium electrode as the mechanism behind the peak, which was also verified by experiments with a thin Pd layer as an electrode. In a glucose free electrolyte surface oxide formation passivates the Pd surface. With addition of glucose the oxide is partially consumed enabling dissolution of the electrode.

In a typical measurement in our study (Pd sheet electrode, ph 5.3, 0.11 M glucose, 5 g/L NaCl, 0.1 V/s scan speed), the specifically dissolved Pd amounts to roughly 9 nmol/cm^2 per scan.

Conflict of interest

We declare no conflict of interest.

Acknowledgements

This work has been supported by the Federal Ministry of Science, Research and Economy (BMWFW), the Federal Ministry of Traffic, Innovation and Technology (bmvit), the Styrian Business Promotion Agency SFG, the Standortagentur Tirol and ZIT – Technology Agency of the City of Vienna through the COMET-Funding Program managed by the Austrian Research Promotion Agency FFG and Siemens AG Österreich.

References

[1] L.C. Clark, C. Lyons, Annals New York Acad. Sci. 102 (1) (1962) 29.
[2] S. Park, H. Boo, T.D. Chung, Analy. Chim. Acta 556 (1) (2006) 46–57.
[3] K.E. Toghill, R.G. Compton, Int. J. Electrochem. Sci. 5 (9) (2010) 1246–1301.
[4] G. Wang et al., Microchim. Acta 180 (3–4) (2013) 161–186.
[5] X. Chen et al., Microchim. Acta (2013) 1–17.
[6] D.W. Kimmel et al., Anal. Chem. 84 (2) (2012) 685–707.
[7] K. Tian, M. Prestgard, A. Tiwari, Mater. Sci. Eng. C-Mater. Biol. Appl. 41 (2014) 100–118.
[8] S. Hermans, A. Deffernez, M. Devillers, Appl. Catal. a-Gen. 395 (1–2) (2011) 19–27.
[9] S. Dash, N. Munichandraiah, J. Electrochem. Soc. 160 (11) (2013) H858–H865.
[10] H. Jeong, J. Kim, Electrochim. Acta 80 (2012) 383–389.
[11] T. Hayashi et al., Anal. Sci. 28 (2) (2012) 127–133.
[12] Y. Zhang et al., Sens. Actuat. B: Chem. 191 (2014) 86–93.
[13] A.L. Sun, J.B. Zheng, Q.L. Sheng, Electrochim. Acta 65 (2012) 64–69.
[14] Q.Y. Wang et al., Rsc Adv. 2 (15) (2012) 6245–6249.
[15] V.Y. Doluda et al., Green Process. Synth. 2 (1) (2013) 25–34.
[16] X.J. Bo et al., Sens. Actuat. B-Chem. 157 (2) (2011) 662–668.
[17] S.J. Guo et al., Acs Nano 4 (7) (2010) 3959–3968.
[18] M.F.L. Demele, H.A. Videla, A.J. Arvia, J. Electrochem. Soc. 129 (10) (1982) 2207–2213.
[19] Y.B. Vassilyev, O.A. Khazova, N.N. Nikolaeva, J. Electroanal. Chem. 196 (1) (1985) 105–125.
[20] Y.B. Vassilyev, O.A. Khazova, N.N. Nikolaeva, J. Electroanal. Chem. 196 (1) (1985) 127–144.
[21] S. Ernst, J. Heitbaum, C.H. Hamann, J. Electroanal. Chem. 100 (1–2) (1979) 173–183.
[22] N.D. Lourenco et al., Anal. Bioanal. Chem. 404 (4) (2012) 1211–1237.
[23] S. Tosi et al., Biotechnol. Prog. 19 (6) (2003) 1816–1821.
[24] E.A. Baldwin et al., Sensors 11 (5) (2011) 4744–4766.
[25] P. Ciosek, W. Wróblewski, Sensors 11 (5) (2011) 4688–4701.
[26] L. Escuder-Gilabert, M. Peris, Anal. Chim. Acta 665 (1) (2010) 15–25.
[27] A. Rudnitskaya, A. Legin, J. Indust. Microbiol. Biotechnol. 35 (5) (2008) 443–451.
[28] M. del Valle, Int. J. Electrochem. 2012 (2012).
[29] M. Gerstl, M. Joksch, G. Fafilek, J. Anal. Bioanal. Tech. S 12 (2013) 2.
[30] B. Beden et al., Electrochim. Acta 41 (5) (1996) 701–709.
[31] A. Damjanov, V. Brusic, Electrochim. Acta 12 (6) (1967). 615-000.
[32] M. Arenz et al., Surf. Sci. 523 (1–2) (2003) 199–209.
[33] L. Meng et al., Anal. Chem. 81 (17) (2009) 7271–7280.
[34] M. Grden et al., Electrochim. Acta 53 (26) (2008) 7583–7598.
[35] A.J. Zhang, M. Gaur, V.I. Birss, J. Electroanal. Chem. 389 (1–2) (1995) 149–159.
[36] M. Seo, M. Aomi, J. Electroanal. Chem. 347 (1–2) (1993) 185–194.
[37] A. Czerwinski, J. Electroanal. Chem. 379 (1–2) (1994) 487–493.
[38] L.H. Dall'Antonia, G. Tremiliosi-Filho, G. Jerkiewicz, J. Electroanal. Chem. 502 (1–2) (2001) 72–81.
[39] A.E. Bolzan, J. Electroanal. Chem. 437 (1–2) (1997) 199–208.
[40] L.D. Burke, Electrochim. Acta 39 (11–12) (1994) 1841–1848.
[41] L.D. Burke, L.C. Nagle, J. Electroanal. Chem. 461 (1–2) (1999) 52–64.
[42] M.W. Breiter, Electrochim. Acta 8 (12) (1963) 925–935.
[43] M.J.N. Pourbaix, J. Van Muylder, N. De Zoubov, Platinum Metals Rev. 3 (2) (1959) 47–53.
[44] M.J.N. Pourbaix, J. Van Muylder, N. De Zoubov, Platinum Metals Rev. 3 (3) (1959) 100–106.
[45] S. Harjanto et al., Mater. Trans. 47 (1) (2006) 129–135.
[46] A.J. Bard et al., Standard potentials in aqueous solution, in: Monographs In Electroanalytical Chemistry and Electrochemistry, first ed., M. Dekker, New York, 1985. xii, pp. 834.